

# Carbon Nanotube-Protein Carriers Enhance Size-Dependent Self-Adjuvant Antibody Response to Haptens.

*Javier Parra*<sup>a</sup>, *Antonio Abad-Somovilla*<sup>b</sup>, *Josep V. Mercader*<sup>a</sup>, *T. Andrew Taton*<sup>c</sup>, and *Antonio Abad-Fuentes*<sup>a,\*</sup>

5

<sup>a</sup> Department of Biotechnology

Institute of Agrochemistry and Food Technology (IATA)

Spanish National Research Council (CSIC)

Agustí Escardino 7, 46980 Paterna, Valencia, Spain

10 E-mail: [aabad@iata.csic.es](mailto:aabad@iata.csic.es)

<sup>b</sup> Department of Organic Chemistry

Universitat de València

Doctor Moliner 50, 46100 Burjassot, Valencia, Spain

15

<sup>c</sup> Department of Chemistry

University of Minnesota

207 Pleasant St. SE, Minneapolis, 55455 Minnesota, USA

20 \* Corresponding author. Department of Biotechnology, Institute of Agrochemistry and Food Technology (IATA), Spanish National Research Council (CSIC), Agustí Escardino 7, 46980 Paterna, Valencia, Spain. Tel.: +34 963 900 022; fax: +34 963 636 301. E-mail: [aabad@iata.csic.es](mailto:aabad@iata.csic.es)

## ABSTRACT

25 Carbon nanotubes (CNTs) are nanomaterials with interesting emerging applications. Their  
properties makes CNTs excellent candidates for use as new nanovehicles in drug delivery,  
immunization and diagnostics. In the current study, we assessed the immune-response-amplifying  
30 properties of CNTs to haptens by using azoxystrobin, the first developed strobilurin fungicide, as a  
model analyte. An azoxystrobin derivative bearing a carboxylated spacer arm (hapten AZc6) was  
covalently coupled to bovine serum albumin (BSA), and the resulting BSA–AZc6 conjugate was  
covalently linked to four functionalized CNTs of different shapes and sizes, varying in diameter and  
length. These four types of CNT-based constructs were obtained using efficient, fast, and easy  
35 functionalization procedures based on microwave–assisted chemistry. New Zealand rabbits and  
BALB/c mice were immunized with BSA–AZc6 alone and with the four CNT–BSA–AZc6  
constructs, both with and without Freund’s adjuvant. The IgG-type antibody responses were assessed  
in terms of the titer and affinity, paying special attention to the relationship between the immune  
response and the size and shape of the employed CNTs. Immunization with CNT–BSA–AZc6  
40 resulted in enhanced titers and excellent affinities for azoxystrobin. More important, remarkable IgG  
responses were obtained even in the absence of an adjuvant, thus proving the self-adjuvanting  
capability of CNTs. Immunogens were able to produce strong anti-azoxystrobin immune responses  
in rabbits even when administered at a BSA–AZc6 conjugate dose as low as 0.05 µg. The short and  
thick CNT–BSA–AZc6 construct produced the best antibody response under all tested conditions.

## KEYWORDS

45 Antigen delivery; Antibodies; Azoxystrobin; Biomaterials; Carbon nanotubes; Immunization

## 1. Introduction

Enhancement of the immune response against antigens is an area of great interest because of its  
50 impact on antibody production. One of the key steps in the immunization process is the phagocytosis  
of the antigen by professional antigen-presenting cells (APCs), such as macrophages, dendritic cells,  
and certain B cells.[1, 2] Once internalized by APCs, the antigen is processed into short peptide  
fragments. The presentation of these peptides by major histocompatibility complex (MHC) class II  
molecules can activate helper T cell responses that ultimately lead to the proliferation of plasma and  
memory B cells and to the production of high-affinity antibodies.[3-6]

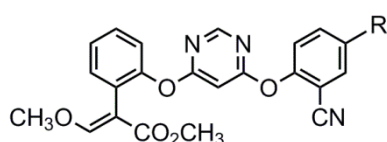
55 The efficiency of the phagocytosis process mainly depends on the size and surface properties of  
the antigen. Large and insoluble particulate antigens are phagocytosed very efficiently and produce  
strong responses by themselves.[7-9] This is the case for microorganisms such as bacteria and  
viruses.[10, 11] Conversely, small and soluble antigens, such as proteins and peptides, are poorly  
internalized and thus weakly immunogenic; therefore, an adjuvant is needed to intensify the immune  
60 response.[12, 13] Triggering an efficient immune response to low-molecular-weight compounds  
(haptens) is an even more challenging task because they are smaller and lack a peptide structure, so  
they cannot be presented by MHC II molecules unless they are conjugated to proteins prior to  
immunization.[14, 15]

65 One of the emerging strategies for increasing the efficiency of the phagocytosis step, thereby  
enhancing the antibody response, is the use of nanomaterials that can increase the size of the antigen  
and modify its surface properties. Micro/nanoparticles (MPs/NPs) have been shown to be well-suited  
for increasing the immune response against protein and peptide antigens because the dimensions of  
particulate systems are comparable to those of microorganisms. Therefore, they can be better  
engulfed by APCs and the antigens can be delivered more efficiently.[16] There are basically two  
70 possible ways to take advantage of MPs/NPs for immunization purposes. One way consists of  
encapsulating the antigen inside liposomes[17, 18] or inside organic biodegradable polymers, such  
as poly(lactic acid) (PLA), poly(lactic-*co*-glycolic acid) (PLGA),[19-24] disulfide cross-linked  
polyacrylates,[25] or polysaccharides, such as pullulan[26] and chitosan.[27-29] This way, the  
particles can easily reach cytosol, where they are degraded, thus releasing the antigen. The other  
75 approach consists of attaching the antigen (covalently or not) to the functionalized surface of  
biocompatible and non-biodegradable particulate materials, such as lecithin NPs,[30] gold NPs,[31-

33] quantum dots,[34] or MPs/NPs based on diverse organic polymers like polystyrene,[35, 36] polypropylene sulfide,[37] or polyacrylate.[38]

Carbon nanotubes (CNTs) are nanomaterials of tubular shape with promising applications in biological and medicinal chemistry.[39-43] They are capable of crossing membranes to penetrate into different types of cells without causing cell death, so both the cell functionality and the activity of the introduced molecules are preserved.[44-46] Based on this finding, CNTs have been successfully employed as nanovehicles for drug delivery[43, 47, 48] and for the transport of biomolecules, such as proteins,[49] peptides,[50] and DNA[42, 51, 52], into cells. Additionally, based on their structural and chemical properties, CNTs can be envisioned as excellent carrier candidates in immunization protocols. They are very hydrophobic and insoluble because of their carbon skeleton structure, and they have a size on the micrometer/nanometer scale, mimicking the properties and size of bacteria. If an antigen is linked to a CNT, the resulting construct could be more easily phagocytosed and rapidly introduced into the immune system, thus improving the antibody response. Pantarotto *et al.*[53, 54] demonstrated the potential of using CNTs for animal immunization. In their seminal work, a peptide from the foot-and-mouth disease virus (FMDV) was covalently coupled to amino-derivatized single-walled carbon nanotubes (SWNTs), and this conjugate was administered to mice. Their results showed that this derivative, together with ovalbumin and an adjuvant, elicited high virus-neutralizing antibody responses in comparison with the non-conjugated peptide. Since this work, the advantages of immunization with proteins and peptides using CNTs have occasionally been confirmed,[55-58] but, to the best of our knowledge, no evidence of an enhancement in the immune response and antibody production against small molecules using CNTs as vehicles has been reported. The production of antibodies displaying high-affinity and specificity to haptens is an important biotechnological research field because tailor-made binders can be used to develop immunoassays and biosensors for targets such as medicinal drugs, pesticides, drugs of abuse, environmental contaminants, food additives, hormones, toxins, etc.

In the present work, we explore for the first time the potential of CNTs as self-adjuvating complexes in order to amplify the antibody response to haptens. Azoxystrobin, a molecule with three aromatic rings interconnected by ether linkages (Chart 1), was selected as the model hapten for this study. Azoxystrobin was the first discovered and patented antifungal of the strobilurin agrochemical family.[59] It is currently the world's best-selling proprietary fungicide with global annual sales over \$1 billion,[60] which makes the development of rapid immunochemical methods for this target a desirable goal. To evaluate the efficiency of CNTs as vehicles for immunization, rabbits and mice were injected with covalent CNT-BSA-hapten constructs. Special attention was paid to the relationship between the antibody response and the CNT size and shape. Animal immunization was carried out with functionalized single- and multi-walled nanotubes (SWNT and MWNT, respectively) that were either shortened or not by an acid oxidative treatment, so four types of CNTs differing in length and diameter were obtained and evaluated. The preparation of this group of functionalized CNTs was performed using fast and easy procedures based on optimized microwave-assisted chemical methods. Finally, the ability of CNTs to efficiently trigger an immune response by themselves, without the need for conventional adjuvants, was also investigated.



**azoxystrobin:** R = H

**hapten (AZc6):** R = (CH<sub>2</sub>)<sub>5</sub>COOH

**Chart 1.** Structure of azoxystrobin and of the AZc6 hapten.

## 125 **2. Materials and methods**

### 2.1. Chemicals and instrumentation

130 Pristine SWNTs (90 wt%, 1-2 nm in diameter, 5-30  $\mu\text{m}$  in length) and MWNTs (95 wt%, 50-80 nm in diameter, 10-20  $\mu\text{m}$  in length) were purchased from Cheap Tubes Inc. (Brattleboro, VT, USA) and used as received. Solvents and reagents for CNT functionalization and for immunogen preparation were obtained from Sigma-Aldrich (St. Louis, MO, USA) and used without further purification. Succinic acid peroxide was obtained from the  $\text{H}_2\text{O}_2$  treatment of succinic acid anhydride, as previously described.[61] The synthesis of hapten AZc6, as well as the preparation and purification of the immunizing BSA–AZc6 conjugate (**5**) and the coating conjugate OVA–AZc6 for the indirect competitive ELISA, has been previously described.[62]

135 Microwave reactions were performed in a CEM Discover S-Class reactor (Matthews, NC, USA) equipped with an infrared pyrometer for temperature control, a pressure control system, magnetic stirring, and a simultaneous air-cooling option. Open vessel reactions were conducted using conventional glassware, whereas pressurized reactions were performed in CEM supplied microwave quartz special vessels. Nylon membranes with a pore size of 0.45  $\mu\text{m}$  were purchased from GE Power & Water (Trevose, PA, USA) for vacuum filtration of CNT samples. The reaction progress was observed by measuring the zeta potential of the samples in deionized water using a Malvern Zetasizer Nano ZS apparatus (Worcestershire, UK). TEM images were obtained using a JEOL 100 kV JEM-1010 microscope (Tokyo, Japan) equipped with a MegaView III digital camera and with the *Analysis* image acquisition software.

145 Azoxystrobin was kindly provided by Syngenta (Basel, Switzerland). Concentrated stock solutions were prepared in anhydrous DMF and stored at  $-20\text{ }^\circ\text{C}$ . Polyclonal goat anti-rabbit IgG–peroxidase antibody (GAR–HRP) was obtained from BioRad (Madrid, Spain). Polyclonal rabbit anti-mouse IgG–peroxidase antibody (RAM–HRP) was obtained from Dako (Glostrup, Denmark). Polyclonal goat anti-mouse IgG–gold antibody (5 nm colloidal gold), *o*-phenylenediamine, complete and incomplete Freund's adjuvants, Tween 20 and other reagents for immunoassays were purchased from Sigma-Aldrich (Madrid, Spain). The preparation of the mouse IgG anti-AZc6 mAb was previously described.[63] Costar 96-well, flat-bottom, high-binding, polystyrene ELISA plates were obtained from Corning (Corning, NY, USA). The microplates were washed using an ELx405 microplate washer from BioTek Instruments (Winooski, VT, USA), and the ELISA absorbances were read using a PowerWave HT reader, also from BioTek Instruments.

### 2.2. Oxidative fragmentation procedure.

160 100 mg of SWNTs or MWNTs were suspended in 25 mL of a 70%  $\text{HNO}_3$  solution in a microwave quartz vessel and sonicated for 15 min. The vessel was closed, and the mixture was irradiated for 30 min at  $190\text{ }^\circ\text{C}$  and at 250 W under a pressure of 19 bar with magnetic stirring and simultaneous air-cooling. Next, the cooled reaction mixture was diluted in 250 mL of deionized water and filtered through a 0.45  $\mu\text{m}$  nylon membrane. The resulting black solid was collected, resuspended in 100 mL of water, sonicated, filtered again, and washed with water. Finally, the air-dried solids were suspended in deionized water at a concentration of 1 mg/mL and sonicated for 5 min to obtain stable solutions of **1a** and **2a** with zeta potential values of  $-35$  and  $-50$  mV, which were stored at  $4\text{ }^\circ\text{C}$ .

### 2.3. Succinic acid peroxide radical insertion procedure.

170 100 mg of SWNTs or 50 mg of MWNTs were suspended in 30 mL of *o*-dichlorobenzene in a conventional round-bottom flask, and 5 g of succinic acid peroxide were added. The mixture was sonicated for 15 min in an ultrasonic bath and then irradiated for 30 min at  $115\text{ }^\circ\text{C}$  and at 250 W under magnetic stirring and simultaneous air-cooling, keeping the vessel open to allow release of the  $\text{CO}_2$  formed. After 15 min of elapsed time, additional succinic acid peroxide (5 g) was added using a solid addition funnel. After cooling, the reaction mixture was diluted with 50 mL of THF, sonicated for 15 min and then filtered through a 0.45  $\mu\text{m}$  nylon membrane. The black solid was collected, suspended in 50 mL of acetone, sonicated, filtered again, and washed with acetone. Finally, the air-dried solids were suspended in deionized water (at a concentration of 1 mg/mL) and sonicated for 5 min to obtain stable suspensions of **3a** and **4a** with zeta potential values of  $-40$  and  $-32$  mV, which were stored at  $4\text{ }^\circ\text{C}$ .

#### 2.4. Synthesis of CNT–NH<sub>2</sub> derivatives **1b** and **3b**.

180 80 mg of CNTs **1a** or **3a** were suspended in a mixture of ethylenediamine and N-methylpyrrolidone (3 mL each) in a microwave quartz vessel and sonicated for 15 min. The reaction vessel was closed, and the mixture was irradiated for 30 min at 190 °C and at 250 W under a pressure of 6 bar with magnetic stirring and simultaneous air-cooling. The cooled reaction mixture was diluted in 20 mL of THF and processed as in the previous procedure. Finally, the black solids obtained were suspended in deionized water at a concentration of 1 mg/mL and briefly sonicated to give stable suspensions of **1b** and **3b** with zeta potential values of +35 mV, which were stored at 4 °C.

#### 2.5. Synthesis of CNT–NH<sub>2</sub> derivatives **2b** and **4b**.

190 50 mg of CNTs **2a** or **4a** were suspended in a mixture of 3 mL of DMSO and 2 mL of N-methylpyrrolidone in a microwave quartz vessel and sonicated for 15 min. The reaction vessel was closed, and the mixture was irradiated for 30 min at 180 °C and at 280 W under a pressure of 6 bar with magnetic stirring and simultaneous air-cooling. The cooled reaction mixture was diluted in 20 mL of THF and processed as previously described to obtain 1 mg/mL aqueous stable dispersions of **2b** and **4b** with zeta potential values of +30 mV, which were stored at 4 °C.

#### 2.6. Synthesis of CNT–BSA–AZc6 immunizing conjugates

195 20 mL of a 0.1 mg/mL solution of conjugate **5** in 100 mM phosphate buffer, pH 7.4, were mixed with 20 mL of a 1 mg/mL solution of each CNT–NH<sub>2</sub> (**1b**, **2b**, **3b**, or **4b**) in deionized water. 180 mg of EDC were added, and the resulting mixture was stirred at room temperature for 2 h. Next, the crude mixture was filtered through a 0.45 µm nylon membrane and washed with water. The black solid was collected, suspended in water, sonicated, filtered again, and washed. This process was repeated three times. Finally, the solids were suspended in water at a concentration of 1 mg/mL by using brief sonication to give stable solutions of the corresponding CNT–BSA–AZc6 derivatives (**1c**, **2c**, **3c**, and **4c**), which showed zeta potential values between –11 and –15 mV. These solutions were stable for a long time when stored at 4 °C.

#### 2.7. Synthesis of CNT–AZc6 (**3d**).

200 100 µL of a 1 mM solution of hapten AZc6 in DMF, 200 mg of EDC, and 20 mg of sulfo–NHS were consecutively added to 20 mL of a 1 mg/mL aqueous solution of **3b** in 100 mM phosphate buffer, pH 7.4, and the resulting mixture was stirred for 2 h at room temperature. The CNT derivative formed (**3d**) showed a zeta potential close to 0 mV and became insoluble in water, so they easily aggregate and precipitate. The crude mixture was filtered through a 0.45 µm nylon membrane and washed, first with water and then with acetone (suspending, sonicating and filtering the solid with each solvent washing). The precipitated conjugate **3d** was stored in water at 4 °C.

#### 2.8. Characterization by immuno–TEM

215 CNT–BSA–AZc6 aqueous solutions were deposited onto grids (a Formvar support film on a copper 400 mesh-grid). After evaporation of the solvent, samples were incubated for 2 h with a 1 µg/mL solution of the specific mouse IgG anti-AZc6 mAb in 1% goat serum, washed three times with Tris-buffered saline, and incubated for 2 h with goat anti–mouse IgG–gold antibody (1/500) in a Tris buffer containing 1% BSA + 0.5% Tween 20. Finally, after several washings with PBS and evaporation of the solvent, the samples were visualized using the TEM microscope.

#### 2.9. Determination of the amount of conjugate **5** attached to the CNTs

225 CNT-based immunogens were diluted in PBS and analyzed in triplicate following the ELISA procedure described below. For this purpose, solutions of CNT constructs were added to the plate in the competitive step with the anti-AZc6 mAb. In the case of CNT–BSA–AZc6 immunogens, standard curves of conjugate **5** in PBS were employed to interpolate the ELISA signals, whereas for the quantification of the hapten AZc6 in **3d** standard curves were prepared using the hapten itself.

230

## 2.10. Animal immunization and antibody production

235 Animal manipulation was performed in compliance with Spanish laws and guidelines (RD  
1201/2005 and law 32/2007) and according to the European Directive 2010/63/EU concerning the  
protection of animals used for scientific purposes. Female BALB/c mice and New Zealand rabbits  
were supplied by Charles River Laboratories (L'Arbresle, France). Rabbits were immunized  
subcutaneously at three-week intervals with the appropriate amount of CNT derivatives. When  
240 adjuvant was used, the CNTs aqueous solution was emulsified with the same volume of complete  
FA for the first injection and of incomplete FA for additional doses. For each injection, a total  
volume of 1 mL was evenly distributed among several sites along the back. When the immunization  
was performed without FA, 1 mL of the CNT derivative in aqueous suspension was administered at  
each injection. Ten days after each dose, a blood sample was taken from the ear vein, and, ten days  
245 after the fourth dose, the animals were exsanguinated by cardiac puncture. Antisera were obtained by  
centrifugation, diluted 1/5 with PBS containing 0.01% thimerosal, and stored at 4 °C in amber vials  
for daily use. For long term storage, the antisera were precipitated twice with ammonium sulfate.

Eight groups of three BALB/c female mice (8–10 weeks old) were immunized at three-week  
intervals by intraperitoneal injections, each group with one of the described CNT–BSA–AZc6  
constructs at the appropriate concentration, with or without FA. Immunogens, essentially prepared as  
250 reported above for rabbits, were administered in a total volume of 200 µL per injection. An  
additional group of mice were immunized with protein conjugate **5** (2 µg) emulsified with FA as a  
control. Antisera were obtained by tail bleeding 10 days after the fourth dose, diluted 1/5 with PBS  
containing 0.01% thimerosal, and stored at 4 °C in amber vials.

## 255 2.11. ELISAs

96-well polystyrene ELISA plates were coated with 100 µL per well of the OVA–AZc6 conjugate  
solution (0.1 µg/mL) in 50 mM carbonate–bicarbonate buffer, pH 9.6, by overnight incubation at  
room temperature. The coated plates were washed four times with washing solution (150 mM NaCl  
containing 0.05% Tween 20), and they received 50 µL per well of the azoxystrobin solution plus 50  
260 µL per well of the mouse or rabbit antisera. From a concentrated azoxystrobin stock solution in  
DMF, calibration curves were prepared in borosilicate glass tubes by serial dilution in PBS. A blank  
was included in each curve. The competitive immunological reaction took place within 1 h at room  
temperature, and the plates were washed again as described. Next, 100 µL per well of the appropriate  
secondary HRP-labeled antibody solution in PBST (PBS containing 0.05% Tween 20) were added,  
265 and the plates were incubated for 1 h at room temperature. In the case of experiments with rabbit  
antisera, a 1/10000 dilution of GAR–HRP was used, whereas with mouse antisera a 1/2000 dilution  
of the RAM–HRP conjugate was employed. After the plates had been washed as described, the  
colorimetric signal was generated by the addition of 100 µL per well of a freshly prepared substrate  
solution (2 mg/mL OPD and 0.012% (v/v) H<sub>2</sub>O<sub>2</sub> in 25 mM citrate and 62 mM phosphate buffer, pH  
270 5.4). The enzymatic reaction was stopped after 10 min at room temperature by adding 100 µL per  
well of 2.5 M sulfuric acid. The absorbance was immediately read at 492 nm, using 650 nm as a  
reference wavelength. Competitive curves were obtained by plotting mean absorbance values *vs.* the  
logarithm of analyte concentration. The resulting sigmoidal curves were fitted to a four-parameter  
logistic equation using the SigmaPlot software package from SPSS Inc. (Chicago, IL). The  
275 antiserum apparent affinity was estimated as the concentration of azoxystrobin at the inflection point  
of the fitted inhibition curve, also referred to as IC<sub>50</sub>. Titer refers to the antiserum dilution that  
produces a maximum absorbance equal to 1.0 under the above described assay conditions.

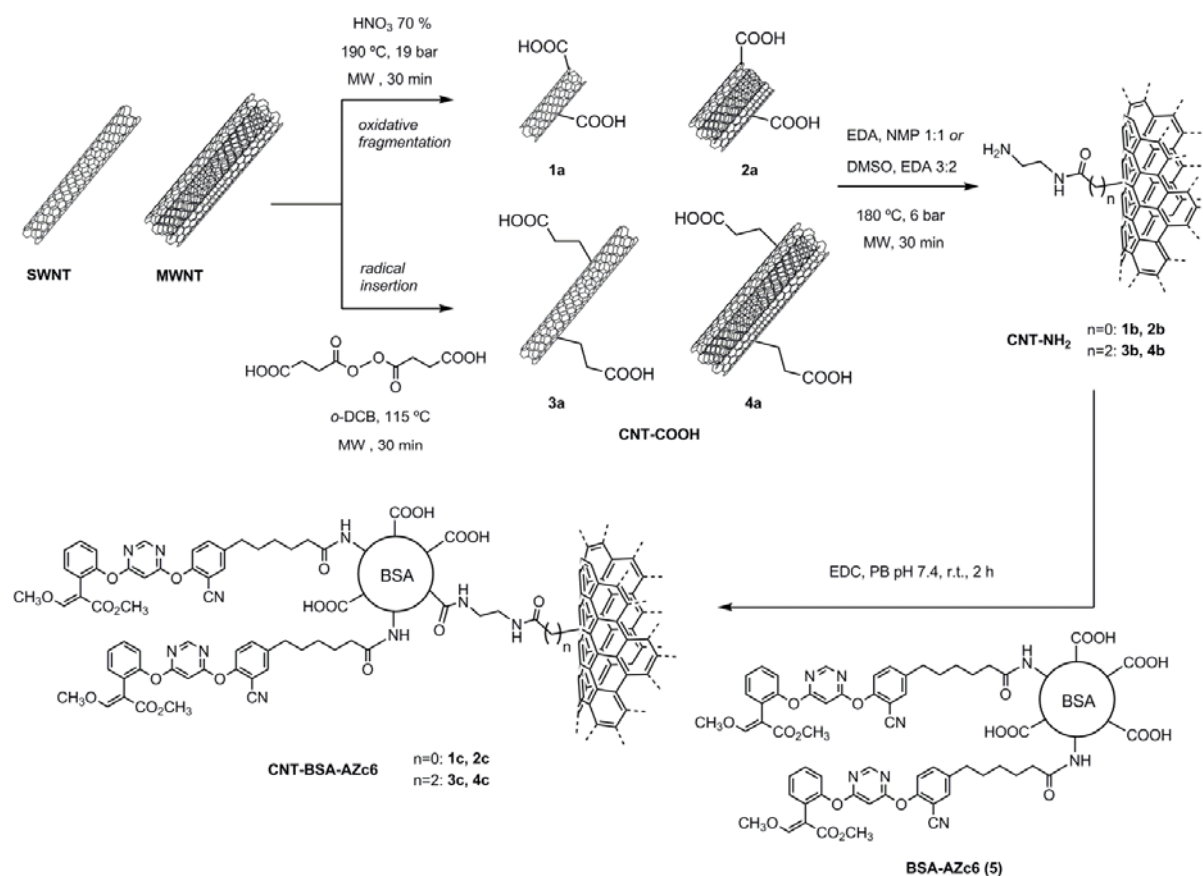
280



### 3. Results and discussion

#### 3.1. Synthesis of the CNT-based immunogens

To assess the relationship between the CNT size and shape and the triggered immune response, four types of CNT–BSA–hapten immunogens, differing in length and diameter, were prepared (Scheme 1): short and thin (**1c**), short and thick (**2c**), long and thin (**3c**), and long and thick (**4c**). Previous studies on the influence of particle size on the cellular uptake and immune response were carried out with nanoparticulate materials, such as PLGA,[64, 65] gold,[31] and polystyrene.[9, 66] Concerning haptens, valuable antibodies have been recently reported using aluminium oxide nanoparticles, nanoparticulated adjuvants, and amphiphilic poly ( $\gamma$ -glutamic acid)[67, 68]. However, similar studies with CNTs and haptens have not been undertaken.



**Scheme 1.** Synthesis of the CNT–BSA–AZc6 constructs **1c**, **2c**, **3c**, and **4c**.

295

Because of the stability and low reactivity of pristine CNTs, their conventional functionalization often requires harsh conditions and reaction times that can take several days. It is well known that CNTs absorb microwave energy because of their structure,[69, 70] allowing them to react more easily when using microwaves than when using conventional heating. In fact, microwave-assisted chemistry has become a very attractive and useful tool for the fast and effective functionalization of CNTs in recent years.[71, 72] Accordingly, synthesis of the four types of CNTs employed in this work was accomplished using pristine SWNTs and MWNTs and rapid, straightforward procedures based on microwave-assisted chemistry. Commercial CNTs are long tubes (5-30  $\mu$ m), and while SWNTs are very thin (1-2 nm), MWNTs are comparatively thick (50-80 nm). We adapted and optimized two general microwave methods in order to functionalize both types of CNTs with adequate moieties for hapten and conjugate coupling, *i.e.*, acid oxidative fragmentation and succinic acid peroxide radical insertion (Scheme 1). The first procedure cuts the CNTs into fragments, inducing the opening of tube caps and the formation of holes in sidewalls. The resulting acid-cut CNT fragments are often less than 1  $\mu$ m in length and include carboxylate moieties at the ends and on the sidewalls of the tubes. On the other hand, radical insertion methods allow the introduction of carboxy-alkyl moieties via a carboxy-alkyl radical attack on the aromatic network of the sidewalls.

310

This way, functional groups are introduced only on the sidewalls, and the length of the CNTs remains essentially unmodified.

315 In the oxidative fragmentation method, SWNTs and MWNTs were treated with concentrated HNO<sub>3</sub> at a high temperature and pressure under microwave irradiation[73] for 30 min. The progress of the carboxylation reaction was observed by measuring changes in the zeta potential values. After the reaction, acid-cut CNTs, **1a** and **2a**, showed excellent solubility in water (up to 1 mg/mL) and zeta potential values of -35 and -50 mV, confirming the existence of numerous negatively charged  
320 carboxylate groups on the CNT surface.

Incorporation of carboxylate functional groups with minor modification of the nanotube length was achieved by using a new microwave-assisted radical insertion method. Previous procedures for introducing alkyl groups into CNTs using radical insertion with acyl peroxides[61, 74-76] often involved long reaction times and/or large amounts of peroxide were consumed. We describe a new  
325 radical insertion method for alkyl chains performed under microwave conditions. Based on previous work by Peng *et al.*,[61] we adapted the conventional heating conditions to efficiently incorporate a carboxyethyl moiety on the sidewalls of SWNTs and MWNTs through a C-C bond. The treatment of pristine CNTs with succinic acid peroxide in *o*-dichlorobenzene at 115 °C under microwave irradiation shortened the reaction time from 10 days to approximately 30 min. Carboxyethyl  
330 functionalized CNTs, **3a** and **4a**, showed a water solubility equivalent to the acid-cut nanotubes and negative zeta potential values of -40 and -32 mV, which indicate adequate functionalization of the CNT sidewall surface.

The next step in the preparation of CNT-based immunogens was the introduction of an ethylenediamine moiety through a covalent amide bond between the available carboxylate groups on the CNT surface and one of the amine groups in ethylenediamine. The synthesis of these types of  
335 derivatives in two steps, using conventional methods, has been previously described.[61, 77] Recently, microwave-assisted protocols have been used in order to achieve this amide bond in CNTs in only one step and without activating reagents.[78-80] Based on the procedure described by Bezdushna *et al.*[81] for the amidation of poly(ether sulfone) carboxylated polymers and starting from **1a** and **3a**, we prepared the amidated SWNTs **1b** and **3b** in a single 30 min step solely using  
340 ethylenediamine and *N*-methylpyrrolidone (Scheme 1). Both types of amidated SWNTs showed zeta potential values of +35 mV. The change in the sign of the zeta potential was indicative of the negatively charged carboxylate residues on the surfaces of the CNTs being substituted by positively charged amine moieties. Like their carboxylated counterparts (CNT-COOH), these amino-aminated  
345 particles (CNT-NH<sub>2</sub>) showed good water solubility, close to 1 mg/mL.

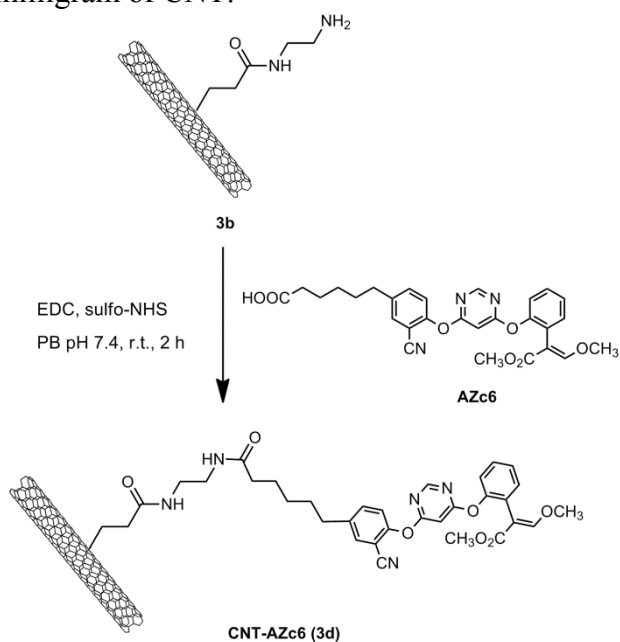
To achieve a direct one-step formation of the amide bond in the carboxylated MWNTs **2a** and **4a**, which showed a much lower reactivity, a better microwave-absorbing solvent (DMSO instead of *N*-methylpyrrolidone) was required. With this solvent change, it was possible to obtain the desired amido-amidated MWNTs **2b** and **4b** with adequate water solubility and zeta potential values (+30  
350 mV in both cases).

Finally, all four types of CNT-NH<sub>2</sub> (**1b**, **2b**, **3b**, and **4b**) were covalently coupled to the protein-hapten conjugate BSA-AZc6 (**5**) via an amide bond between the amine moieties on the surfaces of the CNTs and the available carboxylate groups from the aspartate and glutamate residues in the BSA-hapten conjugate (Scheme 1). Conjugate **5** was prepared[62] with a high hapten-to-protein  
355 molar ratio (MR=26), thus blocking most of the available amine residues in the protein and minimizing protein cross-linking. Conjugate coupling was achieved using standard bioconjugation techniques, *i.e.*, aqueous dispersions of each CNT-NH<sub>2</sub> derivative were mixed with a solution of **5** in phosphate buffer, pH 7.4, in the presence of *N*-(3-dimethylaminopropyl)-*N'*-ethylcarbodiimide (EDC) as a coupling agent. CNT-BSA-AZc6 constructs (**1c**, **2c**, **3c**, and **4c**) showed zeta potential  
360 values between -11 and -15 mV and good solubility in water. Although these properties qualitatively indicated that the coupling reaction had occurred, the amount of **5** attached to the nanotubes was quantified by using an ELISA to confirm this point, employing an anti-AZc6 monoclonal antibody (mAb) previously produced in our lab.[63] Loading values for **5** of approximately 18, 10, 10, and 7 µg per milligram of CNT were calculated for **1c**, **2c**, **3c**, and **4c**,  
365 respectively. Instead of using other common procedures for protein quantification, such as TGA,[72, 76] the Kaiser test for amine residues,[53, 77] or Bradford analysis of the unbound protein,[55] the



ELISA technique was chosen to estimate the protein loading in CNTs because this method gives the amount of conjugate through the interaction with the antibody, thus confirming that the hapten is actually exposed to the environment and therefore free to interact with antibodies and cell receptors during the immune response.

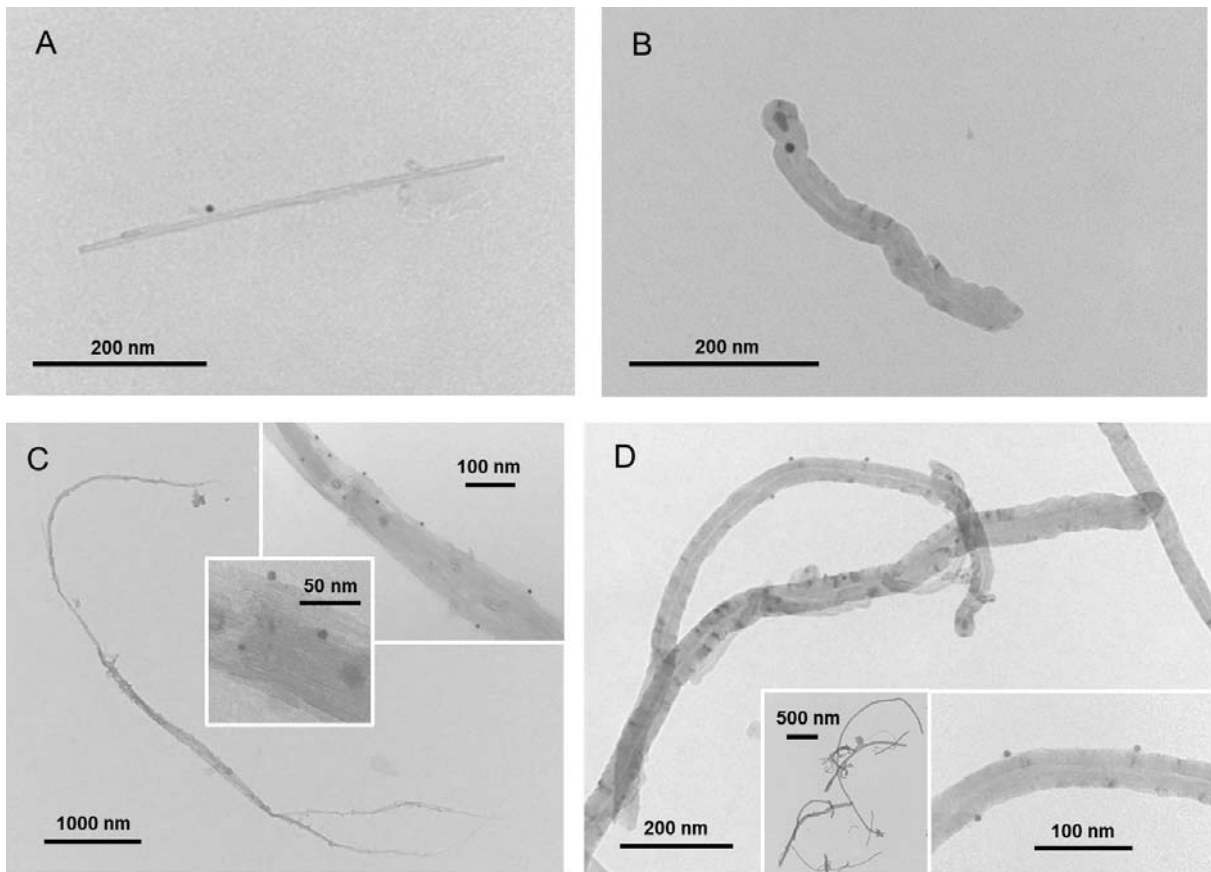
An additional CNT immunogen was prepared which comprised just the hapten AZc6 directly attached to a CNT (**3d**, CNT–AZc6). This construct was used as a negative control based on the widely accepted requirement of a polypeptide in order to produce antibodies against haptens. The hapten AZc6 was conjugated to the amino-aminated SWNT **3b** using EDC and sulfo-NHS as coupling reagents. The immunogen **3d** (Scheme 2) showed a zeta potential value close to 0 mV and very poor water solubility, although it was soluble in DMF at 1 mg/mL. The concentration of AZc6 linked to CNTs, quantified by an ELISA with the anti–AZc6 mAb, was 0.26  $\mu\text{g}$  of hapten per milligram of CNT.



**Scheme 2.** Synthesis of the CNT–AZc6 conjugate (**3d**).

### 3.2. TEM characterization of CNT-based immunogens

Immuno–TEM was carried out to simultaneously characterize the CNT derivatives in terms of size and shape and to image the distribution of the conjugate BSA–AZc6 (**5**) over the CNT walls. Briefly, CNT–BSA–AZc6 particles were labeled with the anti–AZc6 mAb and then incubated with a gold-labeled goat anti-mouse IgG antibody. Fig. 1 shows the immuno-TEM images of the four types of CNT–BSA–AZc6 immunogens. The sharp black dots observed in these photographs confirmed the presence of single molecules of **5** covalently immobilized on the surface of all four types of functionalized CNTs. The TEM images of **1c** and **2c** showed that shortened CNTs that did not exceed 1  $\mu\text{m}$  in length (they were typically between 400 and 600 nm in length; Fig. 1A and 1B), which proved the effectiveness of the acid–oxidation procedure for cutting CNTs into shorter segments. Derivatives **1c** were visualized as individual thin needles 2 nm in diameter (Fig. 1A), whereas **2c** were imaged as individual thick tubular structures approximately 50 nm in diameter (Fig. 1B). For **3c** and **4c**, the TEM images showed longer CNTs several micrometers in length (Fig. 1C and 1D), thus showing that the radical insertion strategy better preserved the original length of the pristine CNTs. In the case of **3c**, the diameter of each individual CNT was approximately 2 nm, but they showed a tendency to group together, forming bundles that can reach up to 100 nm in diameter (Fig. 1C), whereas each individual **4c** showed a diameter of approximately 50 nm (Fig. 1D). Interestingly, an internal small-diameter cylindrical channel can be clearly observed in both **4c** and **2c** derivatives.



**Fig. 1.** Immuno-TEM images of CNT-BSA-AZc6 constructs **1c** (A), **2c** (B), **3c** (C), and **4c** (D).


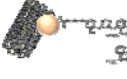
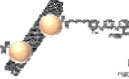


405

### 3.3. Rabbit antibody response with CNT-based immunogens

410

Aqueous solutions of the four CNT-BSA-AZc6 immunogens (**1c**, **2c**, **3c**, and **4c**; Table 1) were subcutaneously administered to rabbits with and without Freund's adjuvant (FA), which is probably the most common adjuvant for antibody production in experimental animals. The volumes were adjusted in order to inoculate the animals with 5  $\mu\text{g}$  of conjugate **5**. CNT-AZc6 (**3d**) emulsified with FA was also injected into control animals. Three additional controls were also employed: 5 and 50  $\mu\text{g}$  of **5** emulsified with adjuvant, and a mixture of 300  $\mu\text{g}$  of **5** with 1 mg/mL of **3b** in phosphate-buffered saline (PBS). It is worthwhile noting that 5  $\mu\text{g}$  is a much lower amount of protein than the most frequently used dose in standard protocols for rabbit immunization (usually 0.1–1 mg).<sup>[82]</sup>

**Table 1.** Main structural features of the CNT–BSA–AZc6 constructs (**1c**, **2c**, **3c**, and **4c**) and the CNT–AZc6 construct (**3d**).

	<b>1c</b>	<b>2c</b>	<b>3c</b>	<b>4c</b>	<b>3d</b>
					
Conjugate loading ( $\mu\text{g } \mathbf{5}/\text{mg CNT}$ )	18	10	10	7	
Hapten loading ( $\mu\text{g } \mathbf{AZc6}/\text{mg CNT}$ )	3.03	1.68	1.68	1.18	0.26
Zeta potential (mV)	-15	-13	-13	-11	0
Functionalization procedure <sup>a</sup>	<i>ox</i>	<i>ox</i>	<i>rad</i>	<i>rad</i>	<i>rad</i>
Solubility in water (1 mg/mL) <sup>b</sup>	+	+	+	+	-
Average dimensions:					
Diameter (nm)	2	50	2 <sup>c</sup>	50	2
Length ( $\mu\text{m}$ )	0.5	0.5	> 2	> 2	>2

<sup>a</sup> Oxidative fragmentation (*ox*) or succinic acid peroxide radical insertion (*rad*).

<sup>b</sup> Solubility in water at 1 mg/mL. Soluble (+) or not soluble (-).

<sup>c</sup> The diameter of each individual **3c** construct is 2 nm, but in the TEM micrographs these tubes tend to aggregate forming bundles that could reach up to 100 nm thick.

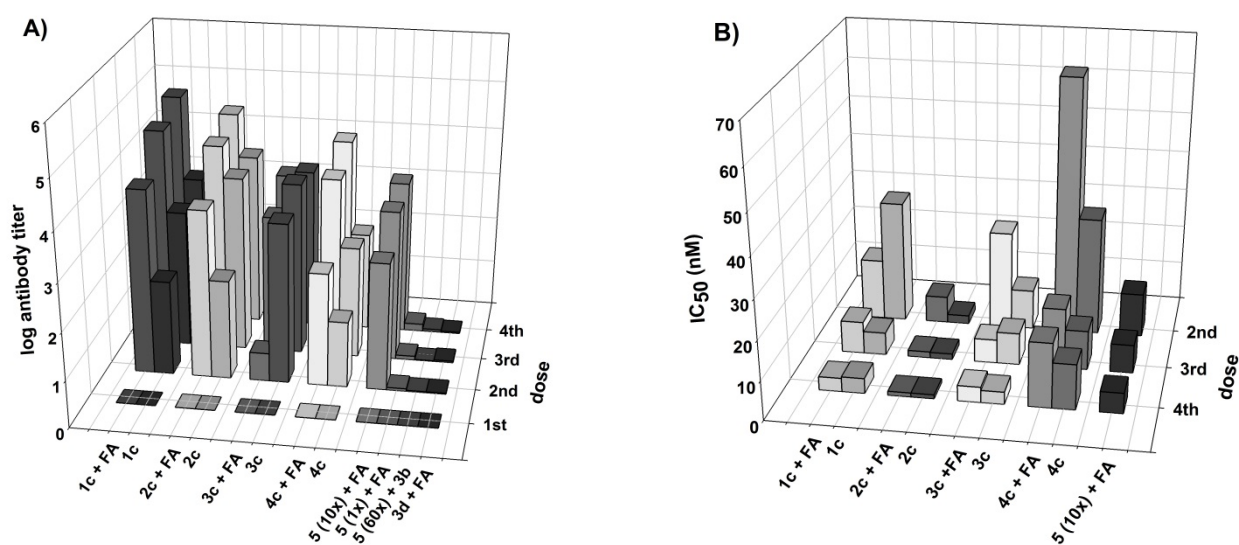
415

The animals received a total of four doses of immunogen. Ten days after each injection they were bled, and the presence of anti-azoxystrobin antibodies in the serum samples was evaluated by ELISA. Fig. 2 shows the evolution of the immune response to azoxystrobin for each immunogen in terms of the antiserum titer (Fig. 2A) and antibody affinity ( $\text{IC}_{50}$ ; Fig. 2B). All four types of CNT-based immunogens were capable of producing IgG responses having outstanding titers and affinities to azoxystrobin. Remarkably, 5  $\mu\text{g}$  of conjugate was unable to trigger a significant response when administered alone, *i.e.*, not attached to CNTs (legend “**5** (1 $\times$ ) + FA” in Fig. 2A). In fact, it was necessary to use an amount of conjugate 10-fold larger (50  $\mu\text{g}$ ) in order to achieve a nearly equivalent output (legend “**5** (10 $\times$ ) + FA” in Fig. 2A). In our opinion, these results showed the practical capability of CNTs for enhancing the immune response against haptens by acting as efficient delivery vehicles. More important, CNTs worked very effectively as immunizing carriers even in the complete absence of FA, as injections with aqueous solutions of CNT–BSA–AZc6 constructs demonstrated. Although slightly lower titers were obtained (Fig. 2A), anti-azoxystrobin antibodies produced from CNT immunogens without FA showed affinities comparable to or even better than those obtained with the positive control (Fig. 2B). Moreover, the fact that the titers gradually increased with booster doses, whereas the  $\text{IC}_{50}$  values decreased down to 1 nM, is indicative of a regular affinity maturation process.

420

425

430



**Fig. 2.** Evolution of the anti-azoxystrobin IgG response in rabbits immunized with 5  $\mu$ g of protein conjugate **5** attached to the different CNT derivatives (**1c**, **2c**, **3c**, and **4c**) with and without FA; 50  $\mu$ g (10x) and 5  $\mu$ g (1x) of **5** + FA (standard procedure); 300  $\mu$ g (60x) of **5** + **3b** (non-covalent mixture of protein conjugate and CNT); and **3d** (0.13  $\mu$ g of hapten AZc6 without carrier protein + FA). A) Evolution of the antibody titer. B) Evolution of the antibody affinity estimated from the IC<sub>50</sub> values obtained from competitive inhibition curves with azoxystrobin standards. Values are the mean of two independent experiments.

To the best of our knowledge, this is the first reported evidence supporting the self-adjuvanting capacity of CNTs for the production of high-affinity antibodies. CNT immunogens are comparable in shape and size to bacteria, so they can be very easily phagocytosed by APCs, which most likely makes the immunostimulatory effect of classical adjuvants unnecessary. This finding has interesting applications for the routine production of antibodies with biotechnological and diagnostic purposes, because immunizations without classical adjuvants are much easier, cheaper, faster, and less painful for animals. The contraindications and negative health effects of the adjuvants employed in animal experimentation, including FA, have been widely described,<sup>[67, 83]</sup> and the painful consequences for the skin are also well known. In our experiments, rabbits showed no skin damage, no wounds, and no apparent negative reactions when subcutaneously injected with CNT constructs in buffer. In line with our results, excellent examples of the production of anti-hapten antibodies using different nanoparticles as safe delivery vehicles have been recently reported for several low molecular weight chemicals.<sup>[67, 68]</sup>


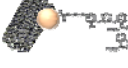
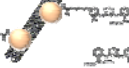

No IgG response against azoxystrobin was observed in rabbits immunized with **3d** + FA (without carrier protein) or with the **5** + **3b** mixture (no covalent linking with the CNT). The absence of a response with **3d** confirms the paradigm that a protein is required for the effective production of anti-hapten antibodies. Although nanoparticles increase the size of the immunogen and allow a better uptake by macrophages, only peptide fragments generated after antigen processing can be linked to MHC II molecules on the APCs surfaces.<sup>[14]</sup> Nevertheless, Maquieira et al. <sup>[68]</sup> have recently reported the existence of a secondary immune response with haptens covalently linked to aluminum oxide nanoparticles, even though further research is probably required to fully clarify the underlying mechanism. On the other hand, the lack of response with the **5** + **3b** mixture shows that non-covalent interactions between the positively charged CNT **3b** and the negatively charged protein conjugate **5** are not sufficient to preserve the integrity of the immunogen; so, a covalent bond between the CNT and the protein-hapten conjugate is needed for proper antigen delivery inside cells.

Finally, Fig. 2 reveals significant differences in the antibody response as a function of CNT size and shape. Our results indicate that CNT vehicles with similar diameters work better if they have shorter lengths. Thus, construct **2c** elicited higher titers and better affinities than **4c**, and **1c** also

evoked higher titers than **3c**, though similar affinities. Construct **4c** turned out to be the worst immunogen, whereas **2c** clearly displayed the best performance, exhibiting the highest titer and the best affinity after the last immunization ( $IC_{50}=1$  nM), both with and without FA.

To gain further insight into the amplifying effect observed for CNT-based constructs, the four immunogens were additionally assessed by immunizing animals with a 10-fold lower amount of protein conjugate **5** (0.5  $\mu$ g per rabbit). Additionally, immunogen **2c** was also evaluated at an even lower dose (0.05  $\mu$ g of conjugate **5**). As shown in Table 2, significant IgG responses were still observed for all four CNT-based immunogens at these low doses (with titers ranging from 1/100 to 1/5000, depending on the type of CNT), whereas no response was observed as before when 5  $\mu$ g of conjugate **5** was administered by conventional protocols, *i.e.*, without being covalently bound to CNTs. Furthermore, titers close to 1/1000 and  $IC_{50}$  values lower than 10 nM were still obtained in rabbits immunized with 0.05  $\mu$ g of **2c**, still the best-performing CNT construct. These results confirm that CNTs could be useful as delivery systems for obtaining strong antibody responses even with antigen amounts 1000-fold lower than typical doses used for rabbit polyclonal antibody production.

**Table 2.** Main immunological features of the CNT-BSA-AZc6 constructs (**1c**, **2c**, **3c**, and **4c**)<sup>a</sup>

		<b>1c</b>	<b>2c</b>	<b>3c</b>	<b>4c</b>
Amount of protein conjugate <b>5</b>					
5 $\mu$ g	Titer (log)	3.1	3.7	3.4	2.1
	$IC_{50}$ (nM)	3.8	1.0	3.1	12.0
5 $\mu$ g + FA	Titer (log)	4.9	4.6	3.3	4.1
	$IC_{50}$ (nM)	3.4	1.0	3.9	16.0
0.5 $\mu$ g + FA	Titer (log)	2.9	3.7	2.3	2.1
	$IC_{50}$ (nM)	9.0	9.6	70.0	20
0.05 $\mu$ g + FA	Titer (log)	n.t. <sup>b</sup>	3.0	n.t.	n.t.
	$IC_{50}$ (nM)	n.t.	7.8	n.t.	n.t.

<sup>a</sup> Rabbit immune response against azoxystrobin after the fourth boost ( $n=2$ ). Results for **3d** are not shown due to the complete lack of response, even when using FA.

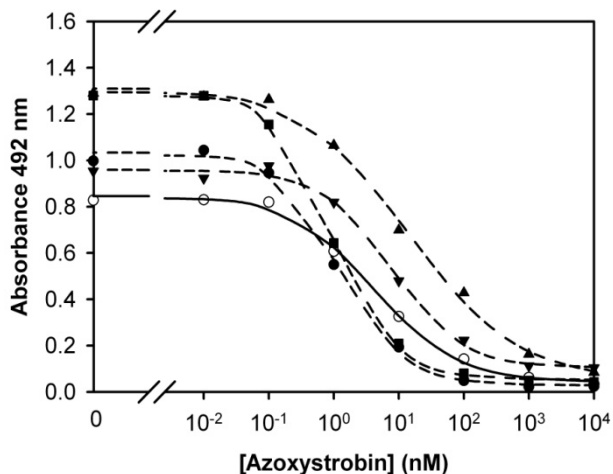
<sup>b</sup> Not tested.

490

Remarkably, azoxystrobin competitive inhibition curves with rabbit antisera obtained from immunogen **2c** at different doses perfectly fitted a four-parameter logistic equation, displaying analytical features equivalent to those of the curve with a rabbit antiserum that was obtained under standard immunization conditions (Fig. 3).

495

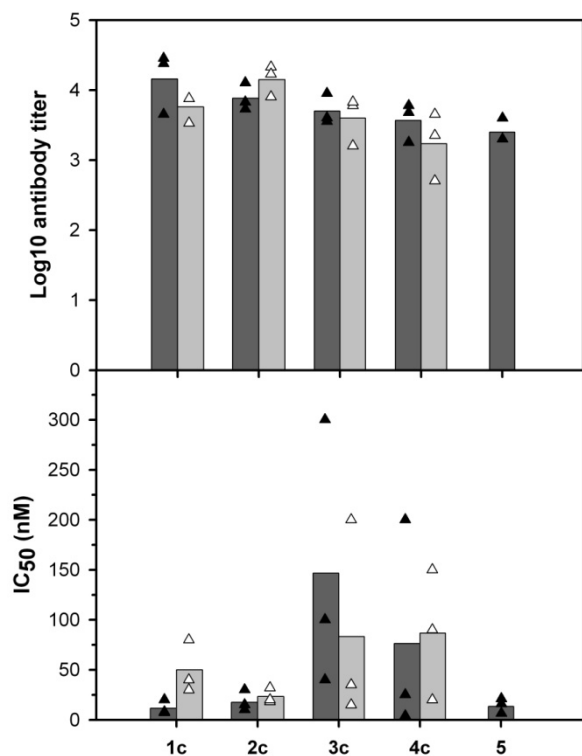




**Fig. 3.** Representative azoxystrobin inhibition curves with rabbit antisera obtained from **2c**. The azoxystrobin standard curve with rabbit antiserum obtained using a standard immunization protocol with 50  $\mu\text{g}$  of **5** in FA ( $\circ$ ) was included as a control. Dashed lines show the azoxystrobin standard curves with rabbit antisera obtained from different amounts of **2c**: ( $\bullet$ ) 5  $\mu\text{g}$  + FA, ( $\blacktriangle$ ) 0.5  $\mu\text{g}$  + FA, ( $\blacktriangledown$ ) 0.05  $\mu\text{g}$  + FA, and ( $\blacksquare$ ) 5  $\mu\text{g}$  without FA (expressed as total content of protein conjugate **5**). Equivalent results were obtained in a replicated independent experiment.

#### 3.4. Mouse antibody response with CNT-based immunogens

Additional immunization experiments were carried out on mice – a widely used animal model for experimental research and particularly for the production of monoclonal antibodies. Groups of 3 mice were immunized intraperitoneally with 2  $\mu\text{g}$  of protein conjugate **5** attached to each CNT derivative, either in aqueous solution or emulsified with FA. As a control, an additional group of 3 mice was immunized with 2  $\mu\text{g}$  of **5** in FA without CNT. Each animal received a total of four injections. Ten days after the fourth dose, blood samples were taken, and the antisera were assessed by ELISA. All of the CNT-based immunogens elicited a strong IgG response, displaying titers even higher than the control, particularly for the shortest particles. This result confirmed **1c** and **2c** as the best constructs for antibody production also in mice and through a different inoculation route (Fig. 4). Moreover, antisera from immunogens **1c** and **2c** also showed superior affinity to the target, with azoxystrobin  $\text{IC}_{50}$  values lower than 50 nM. The most important result emerging from this immunization experiment is the unequivocal capability of CNT-based immunogens to trigger equivalent IgG responses with and without FA, thus further proving the self-adjvanting properties of CNTs.



**Fig. 4.** Titer and affinity of the anti-azoxystrobin IgG response in mice for the four CNT–BSA–AZc6 immunogens after the fourth dose with 2  $\mu$ g of protein conjugate **5** with FA (dark grey bars) and without FA (pale grey bars). The bars are the mean values from three mice immunized with the same construct and the triangles are the individual values for each mouse response.

#### 4. Conclusions

We have employed microwave-assisted procedures to achieve fast and easy covalent functionalization of SWNTs and MWNTs, introducing carboxylate moieties that were subsequently reacted with ethyldiamine to incorporate amine residues. The reactions of these aminated CNTs with protein-hapten conjugate **5** gave the corresponding immunogenic derivatives. The initial application of the radical insertion or oxidative fragmentation methods for both types of pristine CNTs resulted in four types of CNT immunogens, differing in shape and size. The ELISA and immuno-TEM techniques allowed detailed characterization of the prepared immunogens, ensuring that the hapten was properly exposed to the surrounding medium and therefore to the immune system. The obtained antisera displayed excellent titers and affinities to the model hapten, thus showing the capability of CNTs to act as vehicles for enhancing the immune response, even with low amounts of a protein conjugate. This result opens the door to the biotechnological possibility of producing valuable antibodies for other haptens or even whole proteins, particularly if they are difficult to obtain and purify in the quantities required for conventional immunization protocols. Moreover, CNT-based immunogens were able to work very efficiently even without conventional water-in-oil adjuvants, acting as “bacteria-like” antigens with a self-adjuvanting capacity. This finding, beyond its relevance for basic science and its interest as proof-of-concept, could have important practical implications in antibody production because immunization procedures not involving mineral oil adjuvants are faster, cheaper and less painful to animals. Finally, CNT-based immunogens behaved differently depending on the size and shape of their particles. The shorter immunogens (**1c** and **2c**) produced better responses than the longer ones (**3c** and **4c**), most likely because CNTs less than 1  $\mu$ m long are better phagocytosed and engulfed by APCs, although other characteristics associated with the nanoparticle size, such as hydrophobicity and surface antigen density, cannot be discarded. Overall, short and thick CNTs constructs (**2c**) performed optimally as delivery vehicles, producing suitable IgG responses even when loaded with just 0.05  $\mu$ g of the protein conjugate.

## Acknowledgements

This work was supported by *Ministerio de Educación y Ciencia* (AGL2009-12940-C02-01/02/ALI) and cofinanced by FEDER funds. J.P. was hired by *Consejo Superior de Investigaciones Científicas* (CSIC) under a predoctoral *I3P* contract. J.V.M. was also hired by CSIC with a postdoctoral contract under the *Ramón y Cajal* Program. All contracts were cofinanced *Ministerio de Ciencia e Innovación* and the European Social Fund. TEM images were obtained in the SCSIE Microscopy Service of the University of Valencia. We thank Laura López-Sánchez and Ana Izquierdo-Gil for excellent technical assistance.

## References

- [1] A. Savina, S. Amigorena, Phagocytosis and antigen presentation in dendritic cells, *Immunol. Rev.*, 219 (2007) 143-156.
- [2] F.D. Batista, N.E. Harwood, The who, how and where of antigen presentation to B cells, *Nat. Rev. Immunol.*, 9 (2009) 15-27.
- [3] L. Ramachandra, D. Simmons, C.V. Harding, MHC molecules and microbial antigen processing in phagosomes, *Curr. Opin. Immunol.*, 21 (2009) 98-104.
- [4] S. Burgdorf, C. Kurts, Endocytosis mechanisms and the cell biology of antigen presentation, *Curr. Opin. Immunol.*, 20 (2008) 89-95.
- [5] T. Yoshida, H. Mei, T. Doerner, F. Hiepe, A. Radbruch, S. Fillatreau, B.F. Hoyer, Memory B and memory plasma cells, *Immunol. Rev.*, 237 (2010) 117-139.
- [6] M.F. Bachmann, G.T. Jennings, Vaccine delivery: a matter of size, geometry, kinetics and molecular patterns, *Nat. Rev. Immunol.*, 10 (2010) 787-796.
- [7] S.D. Xiang, A. Scholzen, G. Minigo, C. David, V. Apostolopoulos, P.L. Mottram, M. Plebanski, Pathogen recognition and development of particulate vaccines: Does size matter?, *Methods*, 40 (2006) 1-9.
- [8] H. Yue, W. Wei, Z.G. Yue, P.P. Lv, L.Y. Wang, G.H. Ma, Z.G. Su, Particle size affects the cellular response in macrophages, *Eur. J. Pharm. Sci.*, 41 (2010) 650-657.
- [9] C. Foged, B. Brodin, S. Frokjaer, A. Sundblad, Particle size and surface charge affect particle uptake by human dendritic cells in an in vitro model, *Int. J. Pharm.*, 298 (2005) 315-322.
- [10] J.L. Pace, H.A. Rossi, V.M. Esposito, S.M. Frey, K.D. Tucker, R.I. Walker, Inactivated whole-cell bacterial vaccines: current status and novel strategies, *Vaccine*, 16 (1998) 1563-1574.
- [11] A. Detmer, J. Glenting, Live bacterial vaccines - a review and identification of potential hazards, *Microb. Cell Fact.*, 5 (2006).
- [12] Y. Perrie, A.R. Mohammed, D.J. Kirby, S.E. McNeil, V.W. Bramwell, Vaccine adjuvant systems: Enhancing the efficacy of sub-unit protein antigens, *Int. J. Pharm.*, 364 (2008) 272-280.
- [13] J.C. Aguilar, E.G. Rodriguez, Vaccine adjuvants revisited, *Vaccine*, 25 (2007) 3752-3762.
- [14] B.J. McFarland, C. Beeson, Binding interactions between peptides and proteins of the class II major histocompatibility complex, *Med. Res. Rev.*, 22 (2002) 168-203.
- [15] R. Yaneva, C. Schneeweiss, M. Zacharias, S. Springer, Peptide binding to MHC class I and II proteins: New avenues from new methods, *Mol. Immunol.*, 47 (2010) 649-657.
- [16] L.J. Peek, C.R. Middaugh, C. Berkland, Nanotechnology in vaccine delivery, *Adv. Drug Delivery Rev.*, 60 (2008) 915-928.
- [17] C.R. Alving, Liposomes as carriers of antigens and adjuvants, *J. Immunol. Methods*, 140 (1991) 1-13.
- [18] G.F.A. Kersten, D.J.A. Crommelin, Liposomes and iscoms as vaccine formulations, *Biochim. Biophys. Acta*, 1241 (1995) 117-138.
- [19] M. Tafaghodi, A. Khamesipour, M.R. Jaafari, Immunization against leishmaniasis by PLGA nanospheres encapsulated with autoclaved *Leishmania major* (ALM) and CpG-ODN, *Parasitol. Res.*, 108 (2011) 1265-1273.
- [20] C. Thomas, A. Rawat, L. Hope-Weeks, F. Ahsan, Aerosolized PLA and PLGA Nanoparticles Enhance Humoral, Mucosal and Cytokine Responses to Hepatitis B Vaccine, *Mol. Pharm.*, 8 (2011) 405-415.

- 610 [21] S.L. Demento, N. Bonafe, W.G. Cui, S.M. Kaech, M.J. Caplan, E. Fikrig, M. Ledizet, T.M. Fahmy, TLR9-Targeted Biodegradable Nanoparticles as Immunization Vectors Protect against West Nile Encephalitis, *J. Immunol.*, 185 (2010) 2989-2997.
- [22] I. Gutierrez, R.M. Hernandez, M. Igartua, A.R. Gascon, J.L. Pedraz, Influence of dose and immunization route on the serum IgG antibody response to BSA loaded PLGA microspheres, *Vaccine*, 20 (2002) 2181-2190.
- 615 [23] A.K. Hilbert, U. Fritzsche, T. Kissel, Biodegradable microspheres containing influenza A vaccine: Immune response in mice, *Vaccine*, 17 (1999) 1065-1073.
- [24] R.K. Gupta, J. Alroy, M.J. Alonso, R. Langer, G.R. Siber, Chronic local tissue reactions, long term immunogenicity and immunologic priming of mice and guinea pigs to tetanus toxoid encapsulated in biodegradable polymer microspheres composed of poly lactide-co-glycolide polymers, *Vaccine*, 15 (1997) 1716-1723.
- 620 [25] A. Sexton, P.G. Whitney, S.F. Chong, A.N. Zelikin, A.P.R. Johnston, R. De Rose, A.G. Brooks, F. Caruso, S.J. Kent, A Protective Vaccine Delivery System for In Vivo T Cell Stimulation Using Nanoengineered Polymer Hydrogel Capsules, *ACS Nano*, 3 (2009) 3391-3400.
- [26] T. Nochi, Y. Yuki, H. Takahashi, S.I. Sawada, M. Mejima, T. Kohda, N. Harada, I.G. Kong, A. Sato, N. Kataoka, D. Tokuhara, S. Kurokawa, Y. Takahashi, H. Tsukada, S. Kozaki, K. Akiyoshi, H. Kiyono, Nanogel antigenic protein-delivery system for adjuvant-free intranasal vaccines, *Nat. Mater.*, 9 (2010) 685-685.
- 625 [27] S.M. Sivakumar, N. Sukumaran, L. Nirmala, R. Swarnalakshmi, B. Anilbabu, L. Siva, J. Anbu, T.S. Shanmugarajan, V. Ravichandran, Immunopotential of Hepatitis B Vaccine Using Biodegradable Polymers as an Adjuvant, *J. Microbiol. Immunol. Infect.*, 43 (2010) 265-270.
- [28] B. Slutter, S. Bal, C. Keijzer, R. Mallants, N. Hagenaars, I. Que, E. Kaijzel, W. van Eden, P. Augustijns, C. Lowik, J. Bouwstra, F. Broere, W. Jiskoot, Nasal vaccination with N-trimethyl chitosan and PLGA based nanoparticles: Nanoparticle characteristics determine quality and strength of the antibody response in mice against the encapsulated antigen, *Vaccine*, 28 (2010) 6282-6291.
- 635 [29] B. Slutter, L. Plapied, V. Fievez, M.A. Sande, A. des Rieux, Y.J. Schneider, E. Van Riet, W. Jiskoot, V. Preat, Mechanistic study of the adjuvant effect of biodegradable nanoparticles in mucosal vaccination, *J. Control. Release*, 138 (2009) 113-121.
- [30] B.R. Sloat, M.A. Sandoval, A.M. Hau, Y.Q. He, Z.R. Cui, Strong antibody responses induced by protein antigens conjugated onto the surface of lecithin-based nanoparticles, *J. Control. Release*, 141 (2010) 93-100.
- 640 [31] Y.S. Chen, Y.C. Hung, W.H. Lin, G.S. Huang, Assessment of gold nanoparticles as a size-dependent vaccine carrier for enhancing the antibody response against synthetic foot-and-mouth disease virus peptide, *Nanotechnology*, 21 (2010) 195101.
- [32] N. Ishii, F. Fitriawati, A. Manna, H. Akiyama, Y. Tamada, K. Tamada, Gold nanoparticles used as a carrier enhance production of anti-hapten IgG in rabbit: A study with azobenzene-dye as a hapten presented on the entire surface of gold nanoparticles, *Biosci., Biotechnol., Biochem.*, 72 (2008) 124-131.
- 645 [33] D.V. Pow, D.K. Crook, Extremely high-titer polyclonal antisera against small neurotransmitter molecules - rapid production, characterization and use in light-microscopic and electron-microscopic immunocytochemistry, *J. Neurosci. Methods*, 48 (1993) 51-63.
- [34] D. Sen, T.J. Deerinck, M.H. Ellisman, I. Parker, M.D. Cahalan, Quantum Dots for Tracking Dendritic Cells and Priming an Immune Response In Vitro and In Vivo, *Plos One*, 3 (2008).
- [35] D.L.V. Greenwood, K. Dynon, M. Kalkanidis, S. Xiang, M. Plebanski, J.P.Y. Scheerlinck, Vaccination against foot-and-mouth disease virus using peptides conjugated to nano-beads, *Vaccine*, 26 (2008) 2706-2713.
- 655 [36] M. Kalkanidis, G.A. Pietersz, S.D. Xiang, P.L. Mottram, B. Crimeen-Irwin, K. Ardipradja, M. Plebanski, Methods for nano-particle based vaccine formulation and evaluation of their immunogenicity, *Methods*, 40 (2006) 20-29.
- [37] S.T. Reddy, A.J. van der Vlies, E. Simeoni, V. Angeli, G.J. Randolph, C.P. O'Neill, L.K. Lee, 660 M.A. Swartz, J.A. Hubbell, Exploiting lymphatic transport and complement activation in nanoparticle vaccines, *Nat. Biotechnol.*, 25 (2007) 1159-1164.

- [38] M. Skwarczynski, M. Zaman, C.N. Urbani, I.C. Lin, Z.F. Jia, M.R. Batzloff, M.F. Good, M.F. Monteiro, I. Toth, Polyacrylate Dendrimer Nanoparticles: A Self-Adjuvanting Vaccine Delivery System, *Angew. Chem., Int. Ed.*, 49 (2010) 5742-5745.
- 665 [39] K. Kostarelos, A. Bianco, M. Prato, Promises, facts and challenges for carbon nanotubes in imaging and therapeutics, *Nat. Nanotechnol.*, 4 (2009) 627-633.
- [40] A. Bianco, K. Kostarelos, C.D. Partidos, M. Prato, Biomedical applications of functionalised carbon nanotubes, *Chem. Commun.*, (2005) 571-577.
- [41] M. Prato, K. Kostarelos, A. Bianco, Functionalized carbon nanotubes in drug design and discovery, *Acc. Chem. Res.*, 41 (2008) 60-68.
- 670 [42] N.W.S. Kam, M. O'Connell, J.A. Wisdom, H.J. Dai, Carbon nanotubes as multifunctional biological transporters and near-infrared agents for selective cancer cell destruction, *Proc. Natl. Acad. Sci. U. S. A.*, 102 (2005) 11600-11605.
- [43] C. Fabbro, H. Ali-Boucetta, T. Da Ros, K. Kostarelos, A. Bianco, M. Prato, Targeting carbon nanotubes against cancer, *Chem. Commun.*, 48 (2012) 3911-3926.
- 675 [44] H. Dumortier, S. Lacotte, G. Pastorin, R. Marega, W. Wu, D. Bonifazi, J.P. Briand, M. Prato, S. Muller, A. Bianco, Functionalized carbon nanotubes are non-cytotoxic and preserve the functionality of primary immune cells, *Nano Lett.*, 6 (2006) 1522-1528.
- [45] X. Chen, A. Kis, A. Zettl, C.R. Bertozzi, A cell nanoinjector based on carbon nanotubes, *Proc. Natl. Acad. Sci. U. S. A.*, 104 (2007) 8218-8222.
- 680 [46] N.W.S. Kam, H.J. Dai, Carbon nanotubes as intracellular protein transporters: Generality and biological functionality, *J. Am. Chem. Soc.*, 127 (2005) 6021-6026.
- [47] A. Bianco, K. Kostarelos, M. Prato, Applications of carbon nanotubes in drug delivery, *Curr. Opin. Chem. Biol.*, 9 (2005) 674-679.
- 685 [48] C. Klumpp, K. Kostarelos, M. Prato, A. Bianco, Functionalized carbon nanotubes as emerging nanovectors for the delivery of therapeutics, *Biochim. Biophys. Acta, Biomembr.*, 1758 (2006) 404-412.
- [49] N.W.S. Kam, T.C. Jessop, P.A. Wender, H.J. Dai, Nanotube molecular transporters: Internalization of carbon nanotube-protein conjugates into mammalian cells, *J. Am. Chem. Soc.*, 126 (2004) 6850-6851.
- 690 [50] D. Pantarotto, J.P. Briand, M. Prato, A. Bianco, Translocation of bioactive peptides across cell membranes by carbon nanotubes, *Chem. Commun.*, (2004) 16-17.
- [51] R. Singh, D. Pantarotto, D. McCarthy, O. Chaloin, J. Hoebeke, C.D. Partidos, J.P. Briand, M. Prato, A. Bianco, K. Kostarelos, Binding and condensation of plasmid DNA onto functionalized carbon nanotubes: Toward the construction of nanotube-based gene delivery vectors, *J. Am. Chem. Soc.*, 127 (2005) 4388-4396.
- 695 [52] J. Van den Bossche, W.T. Al-Jamal, B.W. Tian, A. Nunes, C. Fabbro, A. Bianco, M. Prato, K. Kostarelos, Efficient receptor-independent intracellular translocation of aptamers mediated by conjugation to carbon nanotubes, *Chem. Commun.*, 46 (2010) 7379-7381.
- 700 [53] D. Pantarotto, C.D. Partidos, R. Graff, J. Hoebeke, J.P. Briand, M. Prato, A. Bianco, Synthesis, structural characterization, and immunological properties of carbon nanotubes functionalized with peptides, *J. Am. Chem. Soc.*, 125 (2003) 6160-6164.
- [54] D. Pantarotto, C.D. Partidos, J. Hoebeke, F. Brown, E. Kramer, J.P. Briand, S. Muller, M. Prato, A. Bianco, Immunization with peptide-functionalized carbon nanotubes enhances virus-specific neutralizing antibody responses, *Chem. Biol.*, 10 (2003) 961-966.
- 705 [55] M. Zeinali, M. Jammalan, S.K. Ardestani, N. Mosaveri, Immunological and cytotoxicological characterization of tuberculin purified protein derivative (PPD) conjugated to single-walled carbon nanotubes, *Immunol. Lett.*, 126 (2009) 48-53.
- [56] J. Meng, J.H. Duan, H. Kong, L. Li, C. Wang, S.S. Xie, S.C. Chen, N. Gu, H.Y. Xu, X.D. Yang, Carbon nanotubes conjugated to tumor lysate protein enhance the efficacy of an antitumor immunotherapy, *Small*, 4 (2008) 1364-1370.
- 710 [57] N. Yandar, G. Pastorin, M. Prato, A. Bianco, M.E. Patarroyo, J.M. Lozano, Immunological profile of a *Plasmodium vivax* AMA-1 N-terminus peptide-carbon nanotube conjugate in an infected *Plasmodium berghei* mouse model, *Vaccine*, 26 (2008) 5864-5873.



- 715 [58] C.H. Villa, T. Dao, I. Ahearn, N. Fehrenbacher, E. Casey, D.A. Rey, T. Korontsvit, V. Zakhaleva, C.A. Batt, M.R. Philips, D.A. Scheinberg, Single-Walled Carbon Nanotubes Deliver Peptide Antigen into Dendritic Cells and Enhance IgG Responses to Tumor-Associated Antigens, *ACS Nano*, 5 (2011) 5300-5311.
- [59] D.W. Bartlett, J.M. Clough, J.R. Godwin, A.A. Hall, M. Hamer, B. Parr-Dobrzanski, The strobilurin fungicides, *Pest Manage. Sci.*, 58 (2002) 649-662.
- 720 [60] For azoxystrobin sales visit the Syngenta web site at:  
[http://www2.syngenta.com/en/investor\\_relations/index.html](http://www2.syngenta.com/en/investor_relations/index.html)
- [61] H.Q. Peng, L.B. Alemany, J.L. Margrave, V.N. Khabashesku, Sidewall carboxylic acid functionalization of single-walled carbon nanotubes, *J. Am. Chem. Soc.*, 125 (2003) 15174-15182.
- 725 [62] J. Parra, J.V. Mercader, C. Agulló, A. Abad-Fuentes, A. Abad-Somovilla, Concise and modular synthesis of regioisomeric haptens for the production of high-affinity and stereoselective antibodies to the strobilurin azoxystrobin, *Tetrahedron*, 67 (2011) 624-635.
- [63] J. Parra, J.V. Mercader, C. Agullo, A. Abad-Somovilla, A. Abad-Fuentes, Generation of anti-azoxystrobin monoclonal antibodies from regioisomeric haptens functionalized at selected sites and development of indirect competitive immunoassays, *Anal. Chim. Acta*, 715 (2012) 105-112.
- 730 [64] I. Gutierrez, R.M. Hernandez, M. Igartua, A.R. Gascon, J.L. Pedraz, Size dependent immune response after subcutaneous, oral and intranasal administration of BSA loaded nanospheres, *Vaccine*, 21 (2002) 67-77.
- [65] C. Thomas, V. Gupta, F. Ahsan, Particle Size Influences the Immune Response Produced by Hepatitis B Vaccine Formulated in Inhalable Particles, *Pharm. Res.*, 27 (2010) 905-919.
- 735 [66] J.A. Champion, A. Walker, S. Mitragotri, Role of particle size in phagocytosis of polymeric microspheres, *Pharm. Res.*, 25 (2008) 1815-1821.
- [67] S.E. George, C.T. Elliott, D.P. McLaughlin, P. Delahaut, T. Akagi, M. Akashi, T.L. Fodey, An investigation into the potential use of nanoparticles as adjuvants for the production of polyclonal antibodies to low molecular weight compounds, *Vet. Immunol. Immunopathol.*, 149 (2012) 46-53.
- 740 [68] A. Maquieira, E.M. Brun, M. Garces-Garcia, R. Puchades, Aluminum Oxide Nanoparticles as Carriers and Adjuvants for Eliciting Antibodies from Non-immunogenic Haptens, *Anal. Chem.*, 84 (2012) 9340-9348.
- [69] T.J. Imholt, C.A. Dyke, B. Hasslacher, J.M. Perez, D.W. Price, J.A. Roberts, J.B. Scott, A. Wadhawan, Z. Ye, J.M. Tour, Nanotubes in Microwave Fields: Light Emission, Intense Heat, Outgassing, and Reconstruction, *Chem. Mater.*, 15 (2003) 3969-3970.
- 745 [70] Z. Ye, W.D. Deering, A. Krokhn, J.A. Roberts, Microwave absorption by an array of carbon nanotubes: A phenomenological model, *Phys. Rev. B*, 74 (2006) 075425.
- [71] N. Rubio, M.A. Herrero, A. de la Hoz, M. Meneghetti, M. Prato, E. Vazquez, Versatile microwave-induced reactions for the multiple functionalization of carbon nanotubes, *Org. Biomol. Chem.*, 8 (2010) 1936-1942.
- 750 [72] F.G. Brunetti, M.A. Herrero, J.D. Munoz, A. Diaz-Ortiz, J. Alfonsi, M. Meneghetti, M. Prato, E. Vazquez, Microwave-induced multiple functionalization of carbon nanotubes, *J. Am. Chem. Soc.*, 130 (2008) 8094-8100.
- 755 [73] Y. Tsukahara, T. Yamauchi, T. Kawamoto, Y. Wada, Functionalization of multi-walled carbon nanotubes realized by microwave-driven chemistry inducing dispersibility in liquid media, *Bull. Chem. Soc. Jpn.*, 81 (2008) 387-392.
- [74] Y.M. Ying, R.K. Saini, F. Liang, A.K. Sadana, W.E. Billups, Functionalization of carbon nanotubes by free radicals, *Org. Lett.*, 5 (2003) 1471-1473.
- 760 [75] A.A. Koval'chuk, V.G. Shevchenko, A.N. Shegolikhin, P.M. Nedorezova, A.N. Klyamkina, A.M. Aladyshev, Effect of Carbon Nanotube Functionalization on the Structural and Mechanical Properties of Polypropylene/MWCNT Composites, *Macromolecules*, 41 (2008) 7536-7542.
- [76] P. Umek, J.W. Seo, K. Hernadi, A. Mrzel, P. Pechy, D.D. Mihailovic, L. Forro, Addition of carbon radicals generated from organic peroxides to single wall carbon nanotubes, *Chem. Mater.*, 15 (2003) 4751-4755.
- 765 [77] W. Wu, S. Wieckowski, G. Pastorin, M. Benincasa, C. Klumpp, J.P. Briand, R. Gennaro, M. Prato, A. Bianco, Targeted delivery of amphotericin B to cells by using functionalized carbon nanotubes, *Angew. Chem., Int. Ed.*, 44 (2005) 6358-6362.

- 770 [78] Y.B. Wang, Z. Iqbal, S. Mitra, Microwave-induced rapid chemical functionalization of single-walled carbon nanotubes, *Carbon*, 43 (2005) 1015-1020.
- [79] W. Mormann, Y. Lu, X. Zou, R. Berger, Modification and Grafting of Multi-Walled Carbon Nanotubes with Bisphenol-A-polycarbonate, *Macromol. Chem. Phys.*, 209 (2008) 2113-2121.
- [80] S. Huang, T. Liu, W.-D. Zhang, W.C. Tjiu, C. He, X. Lu, Grafting polyamide 6 onto multi-walled carbon nanotubes using microwave irradiation, *Polym. Int.*, 59 (2010) 1346-1349.
- 775 [81] E. Bezdushna, H. Ritter, Microwave promoted polymer analogous amidation and esterification of poly(ether sulfone) bearing free carboxylic groups, *Macromol. Chem. Phys.*, 209 (2008) 1942-1947.
- [82] E. Harlow, D. Lane, *Antibodies. A Laboratory Manual*, Cold Spring Harbor Laboratory, Cold Spring Harbor, 1988.
- 780 [83] A. Batista-Duharte, E.B. Lindblad, E. Oviedo-Orta, Progress in understanding adjuvant immunotoxicity mechanisms, *Toxicol. Lett.*, 203 (2011) 97-105.